

1 **Diversity and metabolic potentials of As(III)-oxidizing bacteria in activated**
2 **sludge**

3
4 Rui Xu^{a,b,c,d,1}, Duanyi Huang^{c,d,1}, Xiaoxu Sun^{a,b}, Miaomiao Zhang^{a,b}, Dongbo Wang^{c,d}, Zhaohui Yang^{c,d}, Feng
5 Jiang^e, Pin Gao^{a,b}, Baoqin Li^{a,b}, Weimin Sun^{a,b,f,g,#}

6 ^a National-Regional Joint Engineering Research Center for Soil Pollution Control and Remediation in South
7 China, Guangdong Key Laboratory of Integrated Agro-environmental Pollution Control and Management,
8 Institute of Eco-environmental and Soil Sciences, Guangdong Academy of Sciences, Guangzhou 510650,
9 China

10 ^b Guangdong-Hong Kong-Macao Joint Laboratory for Environmental Pollution and Control, Guangzhou
11 Institute of Geochemistry, Chinese Academy of Sciences, Guangzhou 510640, China

12 ^c College of Environmental Science and Engineering, Hunan University, Changsha 410082, P.R. China

13 ^d Key Laboratory of Environmental Biology and Pollution Control (Hunan University), Ministry of Education,
14 Changsha 410082, P.R. China

15 ^e Guangdong Provincial Key Lab of Environmental Pollution Control and Remediation Technology, School of
16 Environmental Science and Engineering, Sun Yat-sen University, Guangzhou, China

17 ^f School of Environment, Henan Normal University

18 ^g Key Laboratory of Yellow River and Huai River Water Environment and Pollution Control, Ministry of
19 Education

20 **Running Head:** *Structure and function of As(III)-oxidizing bacteria*

21

22 ¹ These authors contributed equally.

23 [#] Correspondence to Weimin Sun, wmsun@soil.gd.cn

24 808 Tianyuan Road, Guangzhou, Guangdong, China.

25 **Abstract**

26 Biological arsenite (As(III)) oxidation is an important process in the removal of toxic arsenic (As) from
27 contaminated water. However, the diversity and metabolic potentials of As(III)-oxidizing bacteria (AOBs)
28 responsible for As(III) oxidation in wastewater treatment facilities are not well documented. In this study, two
29 groups of bioreactors inoculated with activated sludge were operated under anoxic or oxic conditions to treat
30 As-containing synthetic wastewater. Batch tests of inoculated sludges from the bioreactors further indicated
31 that microorganisms could use nitrate or oxygen as electron acceptors to stimulate biological As(III) oxidation,
32 suggesting the potentials of this process in wastewater treatment facilities. In addition, DNA-based stable
33 isotope probing (DNA-SIP) was performed to identify the putative AOBs in the activated sludge. Bacteria
34 associated with *Thiobacillus* were identified as nitrate-dependent AOBs, while bacteria associated with
35 *Hydrogenophaga* were identified as aerobic AOBs in activated sludge. Metagenomic binning reconstructed a
36 number of high-quality metagenome-assembled genomes (MAGs) associated with the putative AOBs.
37 Functional genes encoding for As resistance, As(III) oxidation, denitrification, and carbon fixation were
38 identified in these MAGs, suggesting their potentials for chemoautotrophic As(III) oxidation. In addition, the
39 presence of genes encoding secondary metabolite biosynthesis and extracellular polymeric substance
40 metabolism in these MAGs may facilitate the proliferation of these AOBs in activated sludge and enhance
41 their capacity for As(III) oxidation.

42 **Importance**

43 AOBs play an important role in the removal of toxic arsenic from wastewater. Most of the AOBs have been
44 isolated from natural environments. However, knowledge regarding the structure and functional roles of
45 As(III)-oxidizing communities in wastewater treatment facilities are not well documented. The combination
46 of DNA-SIP and metagenomic binning provides an opportunity to elucidate the diversity of *in situ* AOBs
47 community inhabited the activated sludges. In this study, the putative AOBs responsible for As(III) oxidation

48 in wastewater treatment facilities were identified, and their metabolic potentials including As(III) oxidation,
49 denitrification, carbon fixation, secondary metabolites biosynthesis, and extracellular polymeric substances
50 metabolisms were investigated. This observation provides an understanding of anoxic and/or oxic AOBs
51 during the A(III) oxidation process in wastewater treatment facilities, which may contribute to the removal of
52 As from contaminated water.

53 **Keywords:** DNA-stable isotope probing; Metagenomic binning; As(III)-oxidizing bacteria;
54 Arsenic-contaminated water; Biological As(III) oxidation

55 **Introduction**

56 Arsenic (As) is a toxic and carcinogenic metalloid belonging to group 15 of the periodic table. It is generally
57 accepted that arsenite (As(III)) and arsenate (As(V)) are the predominant forms of inorganic As in the
58 environment (1). Of these two As species, As(V) is less toxic and mobile than As(III) (1). Chronic exposure to
59 As can cause various adverse health effects to humans (2). It has been estimated that hundreds of millions of
60 people in more than 70 countries are threatened by As pollution (3). High amounts of As in aquifers have been
61 found in various natural environments, such as groundwater and surface water (4-6). Wastewater may also
62 contain a significant amount of As due to the widespread usage of As in herbicides, pesticides, and wood
63 preservatives (4, 5, 7-9). This adds to the contamination of water supplies and poses a global health problem (6,
64 10). Therefore, the removal of As from contaminated water is a critical issue worldwide (3). As(III) oxidation
65 is considered as a key step in the removal of As from the aqueous phases because As(V) is more readily
66 removed by the following units, such as coagulation and precipitation (7-9). It is generally recognized that
67 microbiologically mediated As(III) oxidation is more environmentally friendly than chemical As(III)
68 oxidation and does not generate oxidant residuals and harmful byproducts(11). In fact, many
69 As-contaminated wastewater have been treated by biological As(III) oxidation (9, 11, 12).

70 As(III)-oxidizing bacteria (AOBs) are responsible for biological As(III) oxidation. These bacteria are
71 widespread in the environment (4, 13, 14) and are broadly classified into two categories: heterotrophic AOBs
72 and chemoautotrophic AOBs (15). Heterotrophic As(III) oxidation is a bacterial detoxification process.
73 Heterotrophic As oxidizers can convert As(III) to As(V) but they can not derive major energy for growth from
74 this process (16). In contrast, chemoautotrophic AOBs use As(III) as the electron acceptor and gain energy
75 from As(III) oxidation for CO₂ fixation and cell growth under aerobic (17), nitrate-reducing (14), or
76 chlorate-reducing (18) conditions. Generally, chemoautotrophic AOBs are more beneficial than heterotrophic
77 bacteria for As removal because of their lower nutritional requirements (5, 11, 14, 19). To date, most of the
78 known chemoautotrophic AOBs have been isolated from natural environments, such as pyrite mines (20),
79 As-contaminated soils (13), or lakes (14). However, knowledge regarding As(III)-oxidizing communities in
80 wastewater treatment facilities remains limited. Therefore, it is necessary to elucidate the diversity and
81 metabolic potentials of the *in situ* microbial community responsible for As(III) oxidation in wastewater
82 treatment facilities. The emergence of cultivation-independent techniques, such as DNA-based stable isotope
83 probing (SIP) and omics-related approaches, have been shown to reveal the activities of environmental
84 microorganisms and their metabolic potentials without isolation (21, 22). The analysis of stable
85 isotope-labeled DNA followed by molecular techniques links microbial identities to functions in complex
86 environmental samples (19, 23).

87 In this study, two groups of bioreactors were operated to treat As-containing synthetic wastewater under oxic
88 and anoxic conditions. The phylogeny of putative AOBs that actively participated in As(III) oxidation were
89 identified in the ¹³C-labelled batch incubations. Metagenomic binning was used to reconstruct the
90 metagenome assembled genomes (MAGs) of AOBs from these complex microbial communities. Genomic
91 potentials with regard to As(III) oxidation, carbon fixation, and microbial interactions were investigated in the
92 AOB-associated MAGs. The current study aims to investigate (1) Which microorganism are responsible for

93 As(III) oxidation in activated sludge? (2) What are the metabolic potentials of these AOBs? The results
94 provide an understanding of the diversity and metabolic potentials of AOBs during the As(III) oxidation
95 process in wastewater treatment facilities, which may contribute to the removal of As from contaminated
96 water.

97 **Results**

98 *Performances of the As(III)-oxidizing bioreactors under oxic and anoxic conditions*

99 Two types of lab-scale bioreactors were set up under oxic conditions (RO) and anoxic conditions (RN) to
100 treat As-containing synthetic wastewater (**Figure 1**). As(III) was supplemented as the sole electron donor to
101 these reactors for five operation cycles to select the chemoautotrophs. The concentrations of aqueous As(III)
102 and As(V) were monitored over the course of operation. It was observed that concentrations of As(III)
103 constantly decreased with the concomitant generation of As(V), suggesting that As(III) could be oxidized to
104 As(V) under both oxic and anoxic conditions. Moreover, the As(III) oxidation rates in the two bioreactors had
105 a good linear fit with the pseudo-first-order and pseudo-second-order kinetic models as $R^2 > 0.8$ (in all cases,
106 **Figure S2**). Within the five cycles of As(III) oxidation, the k_1 values of the RO (0.06, 0.62, 0.60, 0.35, and
107 0.86, averaged as 0.50 d^{-1}) were higher than those of the RN (0.04, 0.03, 0.09, 0.09, and 0.09, averaged as 0.07
108 d^{-1}). In addition, the k_2 values of the RO (0.09, 1.42, 1.17, 0.78, and 2.29, averaged as $1.15 \text{ mM}^{-1} \text{ d}^{-1}$) were also
109 higher than those of the RN (0.05, 0.04, 0.11, 0.13, and 0.12, averaged as $0.09 \text{ mM}^{-1} \text{ d}^{-1}$). The kinetic model
110 suggested that the As(III) oxidation rates in the RO were higher than those in the RN as reflected by the higher
111 slopes. In addition, the As(III) oxidation gene (*aioA*) was quantified from DNA extracted from the two
112 bioreactors as a proxy of the potential activity of As(III) oxidation. It is observed that the ratio of the *aioA* gene
113 to 16S rRNA gene in the RO was higher than those in the RN (**Figure S3**), suggesting higher potential of
114 As(III) oxidation in RO than that in RN.

115 *Microbial community in the As(III)-oxidizing bioreactors*

116 Microbial communities in the RO and RN were characterized at the end of cycle 1, cycle 3, and cycle 5, as
117 well as in the raw inoculum sludge. The Bray-Curtis distances based PCoA plots indicated that the microbial
118 communities from the RO samples were distinct from the RN samples (**Figure S4**). This result indicated that
119 redox conditions substantially impacted the innate microbial community. Indeed, different microbial taxa
120 were enriched in the RO and RN bioreactors (**Figure 2**). At the phylum level, Proteobacteria dominated in all
121 of the reactors (over 80%) from cycle 1 to 5, while Chloroflexi (2%–6%) and Bacteroidetes (3%–6%) were the
122 second most dominant phylum in the RN and RO bioreactors, respectively. At the genus level,
123 *Pseudoxanthomonas* dominated in the RN bioreactor, with relative abundances ranging from 5% to 40%,
124 followed by *Pseudomonas* (1%–13%) and *Thermomonas* (4%–8%). Other genera, such as *Thiobacillus*,
125 *Acinetobacter*, and *Nitrosomonas*, had a abundances of less than 1%. In the RO bioreactor, the dominant
126 genera were *Comamonas* (21%–32%), followed by *Stenotrophomonas* (11%–18%), *Hydrogenophaga* (3%–
127 9%), *Delftia* (5%–6%), and *Pseudoxanthomonas* (1%–4%).

128 *Batch tests for the As(III) oxidation*

129 The batch incubations were further established using acclimated activated sludges obtained from the two types
130 of bioreactors and were incubated under oxic and anoxic conditions (**Figure S5**). Under anoxic conditions,
131 As(III) oxidation only occurred in the treatments amended by nitrate and As(III), while no As(III) oxidation
132 was observed in the treatments amended by As(III) only or in the sterile controls. The concentrations of nitrate
133 (NO_3^-) constantly decreased with the concomitant generation of nitrite (NO_2^-). The results suggested that
134 As(III) could be oxidized to As(V) by coupling with the reduction of nitrate. Under oxic conditions, As(III)
135 oxidation was only observed in the treatments amended by oxygen and As(III), while As(III) oxidation did not
136 occur in the absence of oxygen or sterilized treatments.

137 Furthermore, DNA-SIP batch incubations were performed to identify the AOBs by feeding the ^{13}C -labeled
138 $\text{NaH}^{13}\text{CO}_3$ as the sole carbon source. Genomic DNA from different gradient fractions, including the
139 $^{13}\text{CAsN}/^{13}\text{CAsO}$, $^{12}\text{CAsN}/^{12}\text{CAsO}$, and ^{13}CAs treatments, were separated into heavy and light fractions using
140 the CsCl gradient ultracentrifugation. The copy numbers of the 16S rRNA gene were measured across each
141 fraction of these treatments from three time points (i.e., days 7, 15, and 30) (**Figure 3**). The copies of 16S
142 rRNA were initially observed at the maximum relative abundance in the “light fractions (BD values of 1.707 g
143 mL^{-1})” in all treatments at day 7. The “peak” of 16S rRNA gradually shifted to the “heavy fractions” (BD
144 values of $1.73\text{--}1.75\text{ g mL}^{-1}$) in either the $^{13}\text{CAsN}$ or the $^{13}\text{CAsO}$ treatments at latter time points on days 15
145 and 30. This suggested that the AOBs gradually incorporated $\text{NaH}^{13}\text{CO}_3$ under both anoxic and oxic
146 conditions. In a comparison, no significant enrichment of the 16S rRNA genes in the “heavy fractions” was
147 observed in either the $^{12}\text{CAsN}/^{12}\text{CAsO}$ or the ^{13}CAs treatments.

148 *Phylogeny of the AOBs*

149 The genomic DNA of the representative fractions (i.e., “heavy” or “light”) from the three treatments (i.e.,
150 $^{13}\text{CAsN}/^{13}\text{CAsO}$, $^{12}\text{CAsN}/^{12}\text{CAsO}$, and ^{13}CAs) at the three time points (i.e., day 7, 15, and 30) were collected
151 for 16S rRNA amplicon sequencing. Specifically, the bacterial taxa enriched in the heavy fractions of the
152 either $^{13}\text{CAsN}$ or $^{13}\text{CAsO}$ treatments were considered as the putative AOBs because they may have
153 incorporated ^{13}C from the $\text{NaH}^{13}\text{CO}_3$ for autotrophic As(III) oxidation. The details on the sample collections
154 are shown in **Table S1**.

155 The microbial communities of each fraction are shown in **Figure 4**. Under anoxic conditions, bacteria
156 affiliated with *Thiobacillus* were identified as one of the most abundant bacteria in the $^{13}\text{CAsN}_{\text{heavy}}$
157 fractions, suggesting that they may have been responsible for nitrate-dependent As(III) oxidation. The relative
158 abundance of *Thiobacillus* was found to be the highest in the $^{13}\text{CAsN}_{\text{heavy}}$ fractions on day 15 (accounting

159 for 56%) and day 30 (69%). In contrast, the relative abundances of *Thiobacillus* were only 0.4% (day 15) and
160 1% (day 30) in the corresponding $^{13}\text{CAsN}_{\text{light}}$ fractions. Additionally, *Serratia* and *Acidovorax* were also
161 detected in the $^{13}\text{CAsN}_{\text{heavy}}$ fractions but with lower relative abundances (less than 0.6%).

162 Under the oxic conditions, bacteria affiliated with *Hydrogenophaga* dominated in the $^{13}\text{CAsO}_{\text{heavy}}$ fractions,
163 followed by *Serratia*, *Brucella*, and *Stenotrophomonas*. The relative abundances of *Hydrogenophaga*
164 accounted for 9% and 23% in $^{13}\text{CAsO}_{\text{heavy}}$ fractions on day 15 and day 30, respectively. The relative
165 abundances of the other genera only accounted for a small proportion, such as *Serratia* (1%–3%), *Brucella*
166 (0.2%–2%), and *Stenotrophomonas* (2%–3%). Notably, *Serratia* were detected in the heavy fractions of both
167 $^{13}\text{CAsN}$ and $^{13}\text{CAsO}$, suggesting that they may be capable of oxidizing As(III) under two redox conditions. In
168 addition, the putative AOBs identified by the DNA-SIP, *Thiobacillus* and *Hydrogenophaga*, were also
169 identified as the keystone taxa of the bacterial communities in the RN and RO bioreactors, respectively
170 (**Figure 5**). Although their percentages in the bioreactors were relatively low (*Thiobacillus* in RN: <1%,
171 *Hydrogenophaga* in RO: 3%–9%, **Figure 2**), high connection degrees between these two AOBs and other
172 bacteria were observed in the co-occurrence networks, suggesting that they may have played critical
173 ecological roles in both the anoxic and oxic bioreactors.

174 *Metagenomic binning of the AOBs*

175 Four metagenomes from representative heavy and light fractions of either $^{13}\text{CAsN}$ or $^{13}\text{CAsO}$ were assembled
176 by metagenomic binning. Metagenomic binning reconstructed 71 high-quality metagenome-assembled
177 genomes (MAGs) with > 60% completeness and < 10% contamination from the four metagenomes. The
178 coverage, completeness, contamination, abundance, and taxonomy of the qualified MAGs were evaluated
179 (**Table S2, Figures S6 and S7**). Among the recovered MAGs, three MAGs associated with putative AOBs,
180 including *Thiobacillus* sp. (bin.9), *Hydrogenophaga* sp. (bin.59), and *Serratia* sp. (bin.30), were obtained and

181 selected for further investigation.

182 *Metabolic potentials of the AOBs*

183 The functional genes of the MAGs associated with the three AOBs were annotated (**Figure 6**). The key genes
184 involved in the As(III) oxidation, (i.e., *aioA* and *aioB*), were detected, suggesting their capability to oxidize
185 As(III). In addition, genes encoding for As resistance (*ACR3* and *arsBC*) and methylation (*arsM*) were also
186 observed in these MAGs. In contrast, the As(V) respiratory reductase gene (*arrA*) was not detected.

187 Because anoxic As(III) oxidation was coupled with nitrate reduction in this study, the genes responsible for
188 denitrification, including nitrate (NO₃⁻) reduction (*nasAB*, *narGHIJ*, and *napAB*), nitrite (NO₂⁻) reduction
189 (*nirAB*, *nirK*, and *nirS*), nitric-oxide (NO) reduction (*norB* and *norC*), and nitrous-oxide (N₂O) reduction
190 (*nosZ*), were searched for in the MAGs. The MAGs associated with the two anaerobic AOBs (i.e.,
191 *Thiobacillus*-associated bin.9 and *Serratia*-associated bin.30) had all of the necessary genes for denitrification,
192 such as *napAB*, *narG*, *nirK*, *norB*, and *nosZ*. In addition, all three AOB-associated MAGs contained genes
193 encoding for six major carbon fixation pathways, suggesting their capacity for chemoautotrophic growth.

194 In addition, a set of genes encoding for secondary metabolites biosynthesis and extracellular polymeric
195 substance (EPS) biosynthesis, regulation, and secretion were investigated in the three AOB-associated MAGs
196 (**Figure 6**). Details on the detected genes can be found in **Tables S2 and S3**. For the secondary metabolite
197 biosynthesis, genes encoding dihydroantcapsin dehydrogenase (*bacC*), 1-deoxy-11beta-hydroxypentalenate
198 dehydrogenase (*ptlF*), and secoisolariciresinol dehydrogenase (*SDH*) were ubiquitously identified in the three
199 AOB-MAGs. Additionally, a number of genes encoding for antibiotic biosynthesis, such as the puromycin
200 biosynthesis protein (*Pur7* and *Pur3*) and bacilysin biosynthesis (*bacF* and *bacG*), were also detected.
201 Additionally, a high abundance of genes involved in EPS metabolism (e.g., glycosyltransferase (*EpsD*),

202 sensor histidine kinase (*KdpD*), glycosyltransferase 2 family protein, and UDP-glucose 4-epimerase) and
203 polysaccharide biosynthesis (polysaccharide biosynthesis proteins (*PslH*, *PslF*, and *PelF*)) were detected in
204 three AOB-associated MAGs.

205 Discussion

206 *Biological As(III) oxidation under different redox conditions*

207 Biological As(III) oxidation driven by AOBs has important environmental implications for treating
208 As-contaminated water. Microbially mediated As(III) oxidation has been extensively studied in natural
209 habitats such as paddy soils (13), sediments (24), and lakes (14). This study further investigated the diversity
210 and metabolic potentials of AOBs inhabiting engineering environments (e.g., activated sludge). Although the
211 activated sludge was inoculated from municipal wastewater treatment plants with low As concentrations, the
212 performances of the two bioreactors indicated that As(III) could be readily oxidized under both anoxic and
213 oxic conditions with the enrichment of AOBs (**Figure 1**). In addition, by fitting the kinetic models, the oxic
214 As(III) oxidation had a relatively higher rate than the anoxic As(III) oxidation (**Figure S2**).

215 As(III) could be oxidized in the wastewater treatment facilities using different electron acceptors. The
216 succession of the electron acceptors for As(III) oxidation generally follows the order of oxygen > nitrate >
217 manganese > iron > sulfate > methanogenesis (25). Dissolved oxygen (DO) may be easily exhausted by
218 various reduced compounds in the bioreactors. Thus, anoxic As(III) may be another important pathway for
219 As(III) oxidation. Given the abundant nitrate in wastewater (26) and the high position of nitrate in the redox
220 tower, microorganisms are likely to use nitrate as electron acceptor to oxidize As(III) in the absence of DO.
221 In this study, the batch incubation further that confirmed the concomitant consumption of As(III) and the
222 generation of As(V) were driven by microorganisms using nitrate or oxygen as the terminal electron acceptors
223 (**Figure S5**). Taken together, these findings suggested that biological As(III) oxidation coupled with the

224 reduction of nitrate or oxygen may have occurred in the As-containing wastewater treatment process.

225 *Putative AOBs and their metabolic potentials*

226 The enrichment of AOBs has successfully promoted the removal of As from many full-scale wastewater
227 treatment plants (7, 9, 11, 27). In this study, the microbial communities inhabiting the RO and the RN were
228 characterized using 16S rRNA gene sequencing (**Figure 2**). A distinct microbial cluster formed during the
229 course of incubation, suggesting that the redox conditions shaped the microbial communities of the activated
230 sludge (**Figure S4**). For instance, *Pseudoxanthomonas* was enriched as the most abundant genus in the RN
231 while *Comamonas* was enriched as the most abundant genus in the RO (**Figure 2B**). However, the
232 dominance of specific taxa in the bioreactors may not indicate that they are responsible for As(III) oxidation
233 (28). For example, He et al. (9) found that *Bacillus* and *Pseudomonas* were the As(III) oxidation related
234 genera, but the percentages of these bacteria in the microbial community were less than 0.1%. Li et al. (11)
235 isolated a number of AOBs from bioreactors and found that their abundances in the bioreactor were low.
236 Therefore, DNA-SIP was used here to identify the phylogeny of the putative AOBs (**Figures 3 and 4**). In our
237 previous work, this method was successfully applied to identify the nitrate-dependent AOBs in paddy soils,
238 such as *Azoarcus*, *Rhodanobacter*, *Pseudomonas*, and Burkholderiales-related bacteria (23). However, none
239 of these AOBs were identified in this study. Instead, bacteria associated with *Thiobacillus* were identified as
240 nitrate-dependent AOBs in sludge, while bacteria associated with *Hydrogenophaga* were identified as aerobic
241 AOBs. *Serratia* spp. were identified as AOBs under both redox conditions, suggesting that the inoculum may
242 also influence the diversity of AOBs.

243 *Thiobacillus* spp. have been previously described as anaerobic denitrifying bacteria with the capability to
244 oxidize Fe(II) (29), FeS (30), and U(IV) oxide minerals (31). Garcia-Dominguez et al. (24) reported that
245 *Thiobacillus* spp. were able to oxidize As(III) aerobically. The current study suggested that *Thiobacillus* is

246 able to anaerobically oxidize As(III) using nitrate as the electron acceptor as well. Metagenomic binning
247 further indicated that a set of key genes involved in As(III) oxidation and denitrification were identified in the
248 *Thiobacillus*-associated bin.9, suggesting their ability to couple As(III) oxidation with nitrate reduction
249 (**Figure 6A**). In addition to As(III) oxidation, genes associated with As resistance were detected in
250 *Thiobacillus*-associated bin.9, which could enable these bacteria to survive under a high concentration of As
251 (32). Moreover, genes encoding six carbon fixation pathways also were identified, suggesting their capability
252 for chemoautotrophic growth.

253 Under oxic conditions, bacteria associated with *Hydrogenophaga* were identified as putative AOBs.
254 *Hydrogenophaga* spp. have been reported to have versatile abilities to oxidize As(III). For example,
255 *Hydrogenophaga* sp. NT-14 was found to heterotrophically oxidize As(III) (33). *Hydrogenophaga* sp. CL-3
256 was able to oxidize As(III) under oxic conditions autotrophically (24). *Hydrogenophaga* sp. H7 can
257 simultaneously oxidize As(III) and degrade aromatic compounds, which is helpful to co-remediate metals and
258 aromatic compounds (34). In addition, members of *Hydrogenophaga* are well known for their capacity for
259 autotrophic growth using CO or hydrogen as electron donors (35). Indeed, the presence of genes encoding
260 As(III) oxidation and carbon fixation further confirmed their roles in autotrophic As(III) oxidation (**Figure**
261 **6B**). In addition, *Serratia* spp. were identified as AOBs under both anoxic and oxic conditions. *Serratia* spp.
262 have been previously identified as putative As(III)-resistant bacteria (36, 37), but have not been reported as
263 AOBs. In this study, a number of genes encoding As resistance, As(III) oxidation, denitrification, and carbon
264 fixation were identified in the *Serratia*-associated bin.30, suggesting their metabolic versatility to
265 autotrophically oxidize As(III) under different redox potentials (**Figure 6C**).

266 *Ecological roles of AOBs in the bacterial community*

267 Given the complexity of the microbial communities residing in activated sludge, it is of great interest to

268 investigate the interactions of these AOBs with other microorganisms inhabiting the sludge. Notably,
269 *Hydrogenophaga* and *Thiobacillus* were identified as “keystone taxa” within the microbial community due to
270 their high connections with other taxa inhabiting the bioreactors (**Figure 5**) (38). These keystone taxa are
271 critical in structuring the microbial interactions and functions by mediating the microbial community
272 composition in response to both environmental and biological factors (38, 39). It has been reported that
273 keystone taxa may use secondary metabolites to regulate other microorganisms in the community (40).
274 Secondary metabolites are small organic molecules produced by an organism that are not necessary for their
275 growth and reproduction, but are responsible for multiple functions in interactions with other organisms in the
276 microbial communities (41). Thus, secondary metabolite production has been suggested to regulate
277 community dynamics (40, 42). Indeed, a number of genes associated with secondary metabolite biosynthesis
278 were observed in these keystone taxa (**Figure 6**). In particular, the detection of genes encoding the
279 biosynthesis of antibiotics here might be important for the successful competition and niche establishment of
280 these AOBs by outcompeting other microorganisms in the bioreactors (**Table S3**). Members of *Thiobacillus*,
281 *Hydrogenophaga*, and *Serratia* have consistently been reported to encode or produce diverse secondary
282 metabolites (43-46). Therefore, further investigation of the metabolic traits of the secondary metabolites
283 synthesized by these “keystone taxa” AOBs could benefit the biological process of As(III) oxidation in
284 wastewater treatment facilities.

285 In addition, a variety of genes encoding key proteins for EPS biosynthesis, regulation, and secretion were
286 detected in these three putative AOBs (**Figure 6** and **Table S4**). EPS is a complex high-molecular-weight
287 mixture of polymers in activated sludge that has a significant influence on the formation of microbial
288 aggregates by providing protective shields (47). The formation of microbial aggregates is an adaptation that
289 enhances the metabolism, survival, and propagation of the microorganisms (48). Likewise, Li et al. (11)
290 enriched the microbial aggregates in biofilm reactors and achieved a higher As(III) oxidation capability and

291 operation stability as compared to those that only used single AOB strains. It is thought that many groups of
292 bacteria coordinate their activities in spatial proximity, which promotes resilience as well as the efficiency of
293 the community. Therefore, the EPS synthesized by AOBs has been suggested to enhance the stability of
294 As(III)-oxidizing communities in activated sludge, which promotes biological As(III) oxidation.

295 In summary, As(III) could be consistently oxidized to As(V) by microorganisms in activated sludge under
296 oxic or anoxic conditions. The biological As(III) oxidation was mediated by AOBs using oxygen or nitrate as
297 the electron acceptors, suggesting the potentials of this process in wastewater treatment facilities.

298 Metagenomic binning reconstructed several high-quality MAGs associated with the putative AOBs, such as
299 *Thiobacillus*, *Hydrogenophaga*, and *Serratia*. The presence of key genes associated with As(III) oxidation, As
300 resistance, denitrification, and carbon fixation in these MAGs suggested their capability for chemoautotrophic
301 As(III) oxidation. In addition, many genes involved in secondary metabolite biosynthesis and EPS metabolism
302 were identified in these MAGs, which may facilitate the proliferation of the AOBs and enhance the As(III)
303 oxidation process. This information provides an understanding of chemoautotrophic AOBs, which may
304 contribute to the removal of As from contaminated water.

305 **Materials and methods**

306 *Sample collection*

307 Fresh sludge was collected from a local wastewater treatment plant (WWTP), which was operated under a
308 conventional activated sludge process. The WWTP received domestic sewage was not contaminated by As.
309 The concentrations of As in the influent and effluent were less than 0.2 mg L⁻¹). The sludge samples were
310 transported to the lab immediately and stored at 4°C for further incubation or analysis.

311 *Operation of the As(III)-oxidizing bioreactors*

312 Two groups of bioreactors were operated in triplicate to treat the As-containing synthetic wastewater
313 (represented by As(III) solution) under anoxic or oxic conditions (1.5 L working volume; **Figure S1, Design**
314 **1**). One group of reactors was purged with N₂ and sealed to create anoxic condition (DO < 0.5 mg L⁻¹, denoted
315 as “RN”). Another group of reactors was purged with compressed air to create oxic condition (DO > 2 mg L⁻¹,
316 “RO”). All of the reactors were seeded with a 100 mL volume of sludge as the inoculum. The RN was fed with
317 synthetic wastewater primarily consisting of 1 mM As(III) and 3 mM nitrate. In comparison, the RO was only
318 fed with 1 mM As(III)-containing synthetic wastewater. All of the reactors were mixed using a magnetic
319 stirrer and equipped with probes to monitor the DO, pH (controlled at 7.0 ± 0.2), and temperature (controlled
320 at 25 ± 1 °C). The effluent of each reactor was collected twice a week to measure the concentrations of As(III)
321 and As(V). Once the As(III) was completely oxidized, the reactors were settled and the supernatant was
322 replaced by fresh As(III)-containing synthetic wastewater (denoted as “one cycle”). A total of five cycles
323 (over 40 days) were conducted. In addition, a kinetic model was calculated to evaluate the oxidation rates
324 based on the pseudo-first-order kinetic model and pseudo-second-order kinetic model. Details of the formula
325 can be found in the supporting information.

326 *DNA extraction from the bioreactors and quantitative PCR*

327 The sludge samples (ca. 2 mL) were collected in triplicate from the RO and RN at the end of running cycle 1
328 (day 15), cycle 3 (day 28), and cycle 5 (day 42). Genomic DNA was immediately extracted from the sludge
329 samples using the FastDNA spin kit (MP Biomedicals, USA) (49). The qualified DNA was sent for 16S rRNA
330 genes sequencing (Illumina MiSeq PE250) to characterize the microbial community composition in the
331 bioreactors (50). The copy number of As(III) oxidation gene (*aiiA*) in the bioreactors were measured using
332 qPCR with the primers aoxBM1-2F/aoxBM2-1R (51). Details of the qPCR mix cocktail can be found in the
333 supporting information.

334 *Batch tests of the As(III) oxidation*

335 The AOB communities in the sludge were expected to be enriched after the long-term operation of the
336 bioreactors, which could be used as acclimated inoculum in batch tests. Two sets of batch tests were
337 established to characterize the biological As(III) oxidation under the control conditions: one was for the
338 As(III)-oxidizing incubation and the other was for the DNA-SIP incubation.

339 *As(III)-oxidizing incubation (Figure S1, Design 2)*: Two types of As(III)-oxidizing incubations were set up to
340 investigate the As(III) oxidation under oxic or anoxic (nitrate-reducing) conditions. The anoxic batch
341 incubations were seeded with acclimatized activated sludge (collected from the RN), NaHCO₃ (as a carbon
342 source), and autoclaved mineral salt medium (MSM) in 100-mL serum bottles (52). The batch bottles were
343 purged with N₂ to exclude oxygen. A total of three anoxic treatments were set up by adding (A) 1 mM As(III)
344 and 3 mM nitrate, and (B) 1 mM As(III) only. Autoclaved controls (C) were also established using sterilized
345 sludge and 1 mM As(III) and 3 mM nitrate additions.

346 For the oxic batch incubation, acclimatized activated sludge (collected from the RO) was mixed with NaHCO₃
347 and MSM in serum bottles as mentioned above. Three oxic treatments were established by adding (A) 1 mM
348 As(III) and constantly purging with compressed air, or (B) 1 mM As(III) only without oxygen. Autoclaved
349 controls (C) were also prepared. For each treatment, triplicate bottles were destructively sampled after 0–7
350 days of incubation. The supernatant was collected for analyses of As(III), As(V), nitrate, and nitrite. Details of
351 the batch incubation and analytical methods can be found in the supporting information.

352 *DNA-SIP incubation (Figure S1, Design 3)*: Batch incubations for DNA-SIP (DNA-SIP incubation) were set
353 up under oxic and anoxic conditions to identify putative AOBs. The DNA-SIP incubations were prepared by
354 mixing 4 mL of the acclimatized activated sludge, 1 mM As(III), and 46 mL of autoclaved MSM under anoxic

355 or oxic conditions. Because aerobic- or nitrate-dependent AOBs utilize HCO_3^- as their carbon source, the
356 assimilation of ^{13}C -labeled $\text{NaH}^{13}\text{CO}_3$ was used to discern the putative AOBs. Two treatments with different
357 terminal electron acceptors were amended by either 8 mM ^{13}C -labeled $\text{NaH}^{13}\text{CO}_3$ (denoted as “ $^{13}\text{CAsN}$ ” for
358 nitrate-dependent or “ $^{13}\text{CAsO}$ ” for oxic), or 8 mM unlabeled $\text{NaH}^{12}\text{CO}_3$ (denoted as “ $^{12}\text{CAsN}$ ” for
359 nitrate-dependent or “ $^{12}\text{CAsO}$ ” for oxic). As a comparison, treatments without terminal electron acceptors
360 were amended by 8 mM ^{13}C -labeled $\text{NaH}^{13}\text{CO}_3$ (denoted as “ ^{13}CAs ”). All of the batch bottles were incubated
361 in the dark and were destructively sampled at days 7, 15, and 30.

362 *DNA extraction from the DNA-SIP gradient fractionation*

363 Genomic DNA was extracted from the DNA-SIP batch incubations from the different treatments (i.e.,
364 $^{13}\text{CAsN}/^{13}\text{CAsO}$, $^{12}\text{CAsN}/^{12}\text{CAsO}$, and ^{13}CAs) at three time points (days 7, 15, and 30). The labelled
365 ^{13}C -DNA and unlabeled ^{12}C -DNA were separated into “heavy” fractions and “light” fractions using CsCl
366 gradient ultracentrifugation. Details of the ultracentrifugation can be found in the supporting information.

367 *Quantitative PCR and high-throughput sequencing of the DNA-SIP gradient fractionation*

368 The relative abundances of 16S rRNA gene copies in each fraction were measured using qPCR. The gene
369 copies were quantified using the primers 338F/518R (53). Details of the qPCR mix cocktail can be found in
370 the supporting information. DNA samples from the representative gradient fractions (e.g., heavy or light
371 fractions) in each treatment were selected for 16S rRNA amplicon sequencing (V4 region with the primer set
372 515F/806R) to characterize the microbial communities. In addition, DNA samples from the representative
373 gradient fractions (e.g., heavy or light fractions) in the either $^{13}\text{CAsN}$ or $^{13}\text{CAsO}$ cultures were sent for shotgun
374 metagenomic sequencing (Illumina Hiseq 4000) (54). Detailed information about the selected fractions for
375 amplicon and shotgun metagenomic sequencing can be found in **Table S1**.

376 *Bioinformatic analysis*

377 Raw amplicon sequencing data (19 samples from bioreactors and 75 samples from the DNA-SIP incubations)
378 were merged, trimmed, and filtered using USEARCH. The non-redundant sequence was denoised to obtain
379 the unique amplicon sequence variants (ASV) for the classification of taxonomy. Details of the analysis can be
380 found in the supporting information.

381 For the shotgun metagenomic sequencing data, a total of four metagenomes with 140 Gb raw reads were
382 initially checked using Trimmomatic for quality control with options “SLIDINGWINDOW:4:20
383 MINLEN:70” (49, 55, 56). The trimmed reads were then evaluated using the FastQC toolkit. The clean data
384 were *de novo* assembled using MEGAHIT (k-mer: 21–121, at the step of 10) (57). Metagenomic binning of
385 the assembled contigs was conducted by MetaWRAP using MetaBAT2, MaxBin2, and CONCOT software
386 (58). The recovered MAGs were refined and reassembled to improve their quality. CheckM was used to retain
387 the qualified MAGs with a completion of > 60% and contamination of < 10% (59, 60). The taxonomy of the
388 MAGs was annotated using the Genome Taxonomy Database (GTDB) (61). The functional genes of the
389 MAGs were annotated using the KofamKOALA with default parameters (62).

390 *Statistical methods*

391 Co-occurrence networks were constructed to explore the microbial correlations within the microbial
392 communities (63). The co-occurrence networks were generated using the Spearman’s correlations with $|R| >$
393 0.6 and $P < 0.05$ in R (“ggcorrplot”) (53). The calculated node-edge pairs were then used to construct the
394 different networks in Gephi v. 0.92 software (64). The node size was proportional to the number of
395 connections (65). Data visualization was performed using GraphPad Prism v. 8.

396 **Figure legends**

397 **Figure 1.** Bioreactor performances under anoxic (RN) or oxic (RO) conditions: (A) concentrations of As(III)
398 and (B) concentrations of As(V). Triplicated bioreactors of each condition were operated for five cycles by
399 feeding with the As(III) synthetic wastewater. The triangles represent the sampling times for the microbial
400 community analysis.

401 **Figure 2.** Microbial communities in the anoxic bioreactors (RN) and oxic bioreactors (RO) for As(III)
402 oxidation: (A) the major phyla (top 5) and (B) the major genera (top 20). Sludge samples were collected in
403 triplicate from the raw inoculum sludge (0 day) and at the end of operation cycle 1 (15 days), cycle 3 (28
404 days), and cycle 5 (42 days).

405 **Figure 3.** 16S rRNA quantification by the quantitative PCR (qPCR) indicated that the As(III)-oxidizing
406 bacteria (AOBs) were labeled in the (A) anoxic and (B) oxic DNA-SIP incubations. The distribution of the
407 16S rRNA genes were normalized to the highest 16S rRNA gene copies. The legends “ $^{13}\text{CAsN}$ ” or “ $^{13}\text{CAsO}$ ”
408 represent the treatments amended with the $\text{NaH}^{13}\text{CO}_3$ and terminal electron acceptors (nitrate for $^{13}\text{CAsN}$ or
409 oxygen for $^{13}\text{CAsO}$). As a comparison, “ $^{12}\text{CAsN}$ ” or “ $^{12}\text{CAsO}$ ” represent the treatments amended with the
410 $\text{NaH}^{12}\text{CO}_3$ and terminal electron acceptors (nitrate for $^{12}\text{CAsN}$ or oxygen for $^{12}\text{CAsO}$). “ ^{13}CAs ” represent the
411 treatment amended with $\text{NaH}^{13}\text{CO}_3$ without any electron acceptors.

412 **Figure 4.** Relative abundances of the bacterial communities (genus level) in the heavy and light fractions
413 from either (A) anoxic or (B) oxic DNA-SIP incubations, including three treatments (i.e., $^{13}\text{CAsN}/^{13}\text{CAsO}$,
414 $^{12}\text{CAsN}/^{12}\text{CAsO}$, and ^{13}CAs) at three time points (i.e., days 7, 15, and 30). The ^{13}C -labeled bacteria
415 represent the putative As(III)-oxidizing bacteria in the $^{13}\text{CAsN}_{\text{heavy}}$ and $^{13}\text{CAsO}_{\text{heavy}}$ fractions, which
416 are highlighted with red bubbles.

417 **Figure 5.** The co-occurrence networks of the bacteria communities in the (A) anoxic bioreactors (RN) and
418 (B) oxic bioreactors (RO). The ^{13}C -labeled As(III)-oxidizing bacteria by DNA-SIP are highlighted with red
419 and navy nodes in the two networks, respectively. The size of the node denotes the connection degree.

420 **Figure 6.** Genes encoding As cycling (blue), denitrification (green), carbon fixation (purple), extracellular
421 polymeric substance (EPS) metabolisms (red), and secondary metabolites (SMs) biosynthesis (yellow) in the
422 three metagenome-assembled genomes (MAGs) associated with the putative As(III)-oxidizing bacteria: (A)
423 *Thiobacillus* sp. (bin.9), (B) *Hydrogenophaga* sp. (bin.59), and (C) *Serratia* sp. (bin.30). The height of the
424 bar indicates the gene abundance.

425 **Acknowledgments**

426 This work was supported by the National Natural Science Foundation of China (Grant Nos. 42007357
427 and 41771301), the China Postdoctoral Science Foundation (Grant No. 2020T130127), the Science and
428 Technology Planning Project of Guangzhou (Grant Nos. 202002030271 and 202002020072), the Guangdong
429 Basic and Applied Basic Research Foundation (Grant No. 2019A1515110351), and the GDAS' Project of
430 Science and Technology Development (Grant No. 2020GDASYL-20200102014). We would like to thank Mr.
431 Tang Yao for donating the sludge samples. We also would like to thank Dr. Cao Jiao for the calculation of the
432 kinetic models.

433 **Conflict of interest**

434 The authors declare they have no conflict of interest to report.

435 **Availability of data**

436 The datasets of the 16S rRNA amplicon sequencing and shotgun metagenomic sequencing generated and

437 analyzed during the current study have been submitted to the NCBI GenBank database with the project
438 number PRJNA713939.

439 **References**

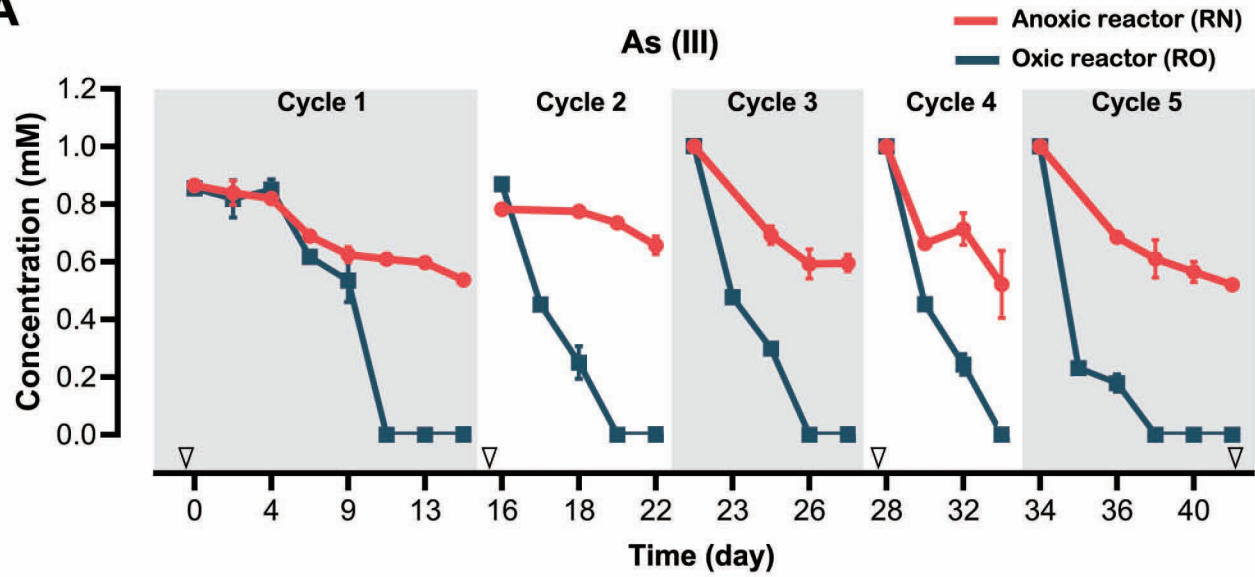
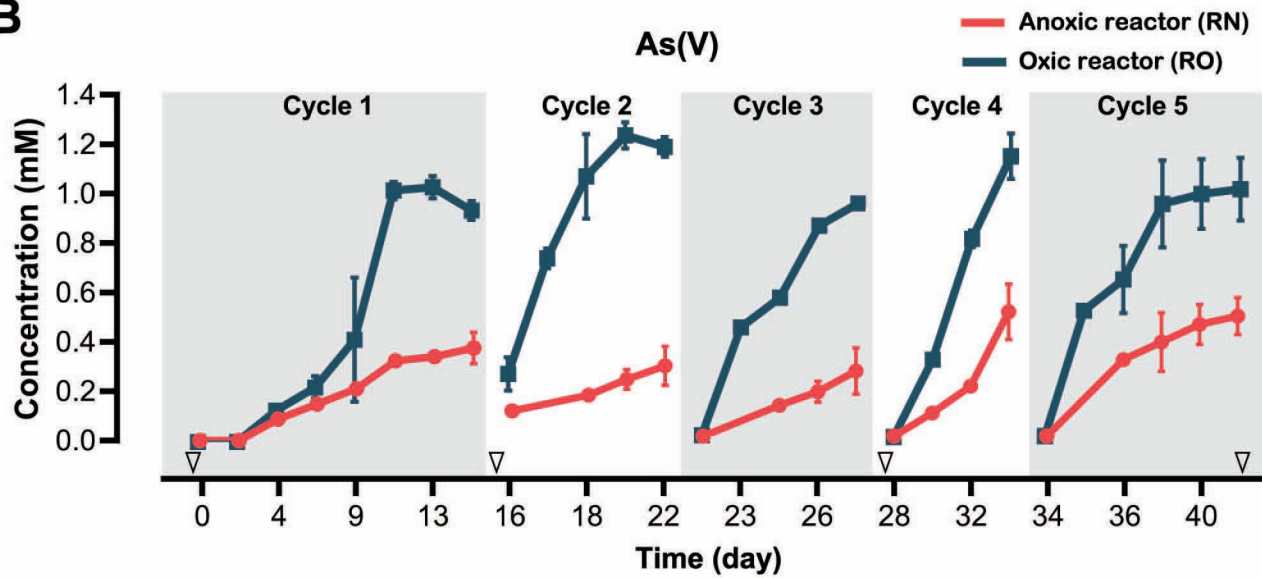
- 440 1. Zhu Y, Xue X, Kappler A, Rosen BP, Meharg AA. 2017. Linking genes to microbial biogeochemical
441 cycling: lessons from arsenic. *Environmental Science & Technology* 51:7326-7339.
- 442 2. Rahman MM, Ng JC, Naidu R. 2009. Chronic exposure of arsenic via drinking water and its adverse
443 health impacts on humans. *Environmental Geochemistry and Health* 31:189-200.
- 444 3. Singh R, Singh S, Parihar P, Singh VP, Prasad SM. 2015. Arsenic contamination, consequences and
445 remediation techniques: a review. *Ecotoxicology and Environmental Safety* 112:247-270.
- 446 4. Sun W, Sierra R, Field JA. 2008. Anoxic oxidation of arsenite linked to denitrification in sludges and
447 sediments. *Water Research* 42:4569-4577.
- 448 5. Lièvremon D, Bertin PN, Lett M-C. 2009. Arsenic in contaminated waters: Biogeochemical cycle,
449 microbial metabolism and biotreatment processes. *Biochimie* 91:1229-1237.
- 450 6. Bhattacharya P, Welch AH, Stollenwerk KG, McLaughlin MJ, Bundschuh J, Panaullah G. 2007. Arsenic
451 in the environment: Biology and Chemistry. *Science of The Total Environment* 379:109-120.
- 452 7. Andrianisa HA, Ito A, Sasaki A, Aizawa J, Umita T. 2008. Biotransformation of arsenic species by
453 activated sludge and removal of bio-oxidised arsenate from wastewater by coagulation with ferric chloride.
454 *Water Research* 42:4809-4817.
- 455 8. Sullivan C, Tyrer M, Cheeseman CR, Graham NJD. 2010. Disposal of water treatment wastes
456 containing arsenic — A review. *Science of The Total Environment* 408:1770-1778.
- 457 9. He Z, Zhang Q, Wei Z, Wang S, Pan X. 2019. Multiple-pathway arsenic oxidation and removal from
458 wastewater by a novel manganese-oxidizing aerobic granular sludge. *Water Research* 157:83-93.
- 459 10. Song P, Yang Z, Zeng G, Yang X, Xu H, Wang L, Xu R, Xiong W, Ahmad K. 2017. Electrocoagulation
460 treatment of arsenic in wastewaters: A comprehensive review. *Chemical Engineering Journal* 317:707-725.
- 461 11. Li H, Zeng X-C, He Z, Chen X, E G, Han Y, Wang Y. 2016. Long-term performance of rapid oxidation
462 of arsenite in simulated groundwater using a population of arsenite-oxidizing microorganisms in a bioreactor.
463 *Water Research* 101:393-401.
- 464 12. Sun W, Sierra-Alvarez R, Hsu I, Rowlette P, Field JA. 2010. Anoxic oxidation of arsenite linked to
465 chemolithotrophic denitrification in continuous bioreactors. *Biotechnology and Bioengineering*
466 105:909-917.
- 467 13. Zhang J, Zhao S, Xu Y, Zhou W, Huang K, Tang Z, Zhao F-J. 2017. Nitrate stimulates anaerobic
468 microbial arsenite oxidation in paddy soils. *Environmental Science & Technology* 51:4377-4386.
- 469 14. Oremland RS, Hoelt SE, Santini JM, Bano N, Hollibaugh RA, Hollibaugh JT. 2002. Anaerobic
470 oxidation of arsenite in Mono Lake water and by a facultative, arsenite-oxidizing chemoautotroph, strain
471 MLHE-1. *Applied and Environmental Microbiology* 68:4795-4802.
- 472 15. Oremland RS, Stolz JF. 2005. Arsenic, microbes and contaminated aquifers. *Trends in Microbiology*

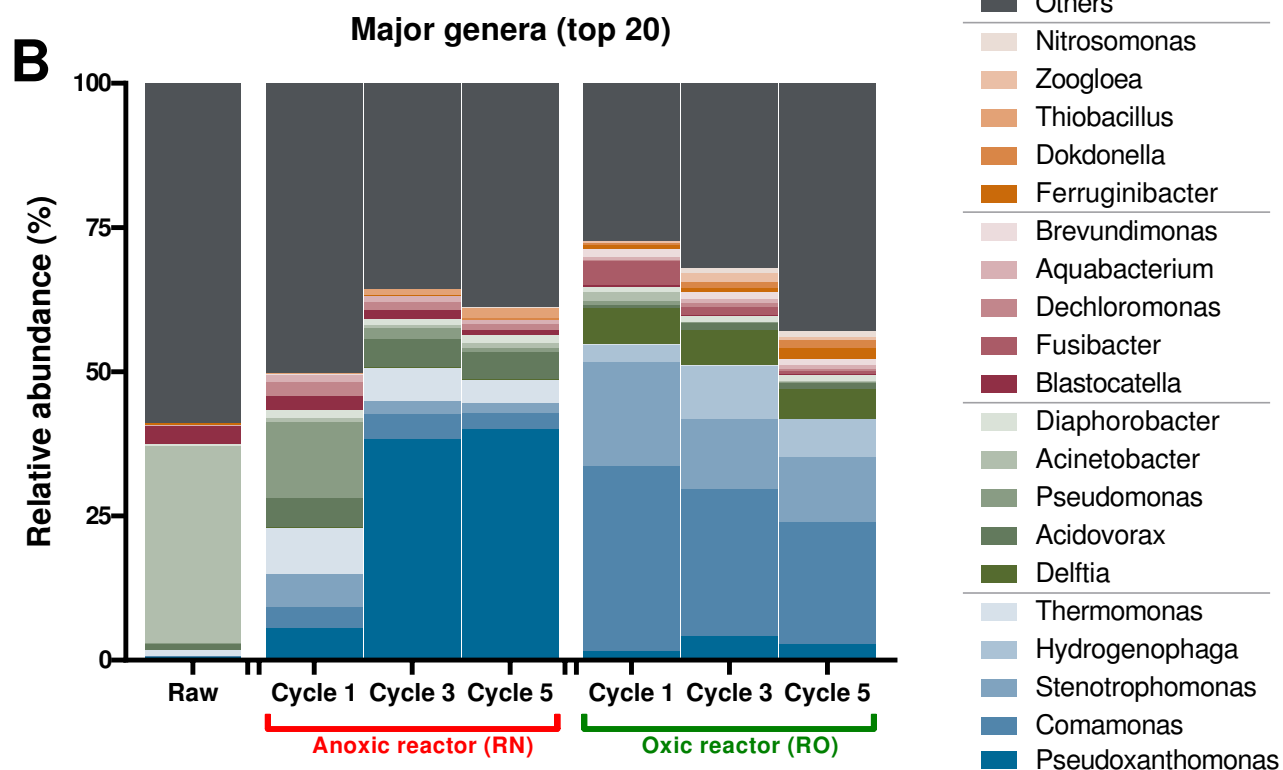
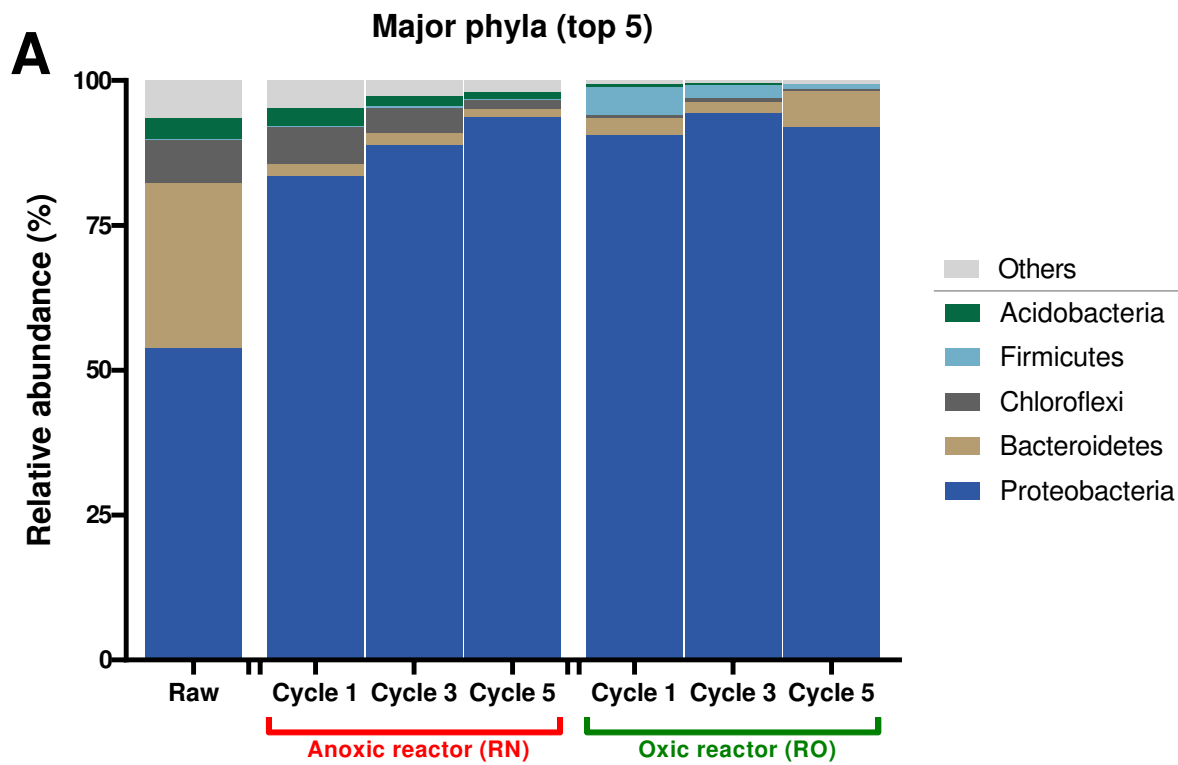
- 473 13:45-9.
- 474 16. Silver S, Phung LT. 2005. Genes and enzymes involved in bacterial oxidation and reduction of inorganic
475 arsenic. *Applied and Environmental Microbiology* 71:599-608.
- 476 17. Inskeep WP, Macur RE, Hamamura N, Warelow TP, Ward SA, Santini JM. 2007. Detection, diversity
477 and expression of aerobic bacterial arsenite oxidase genes. *Environmental Microbiology* 9:934-43.
- 478 18. Sun W, Sierra-Alvarez R, Milner L, Field JA. 2010. Anaerobic oxidation of arsenite linked to chlorate
479 reduction. *Applied and Environmental Microbiology* 76:6804.
- 480 19. Xing W, Li J, Li D, Hu J, Deng S, Cui Y, Yao H. 2018. Stable-isotope probing reveals the activity and
481 function of autotrophic and heterotrophic denitrifiers in nitrate removal from organic-limited wastewater.
482 *Environmental Science & Technology* 52:7867-7875.
- 483 20. Santini JM, Sly LI, Schnagl RD, Macy JM. 2000. A new chemolithoautotrophic arsenite-oxidizing
484 bacterium isolated from a gold mine: phylogenetic, physiological, and preliminary biochemical studies.
485 *Applied and Environmental Microbiology* 66:92-97.
- 486 21. Alneberg J, Bjarnason BS, de Bruijn I, Schirmer M, Quick J, Ijaz UZ, Lahti L, Loman NJ, Andersson
487 AF, Quince C. 2014. Binning metagenomic contigs by coverage and composition. *Nature Methods*
488 11:1144-1146.
- 489 22. Xu R, Sun X, Häggblom MM, Dong Y, Zhang M, Yang Z, Xiao E, Xiao T, Gao P, Li B, Sun W.
490 Metabolic potentials of members of the class Acidobacteriia in metal-contaminated soils revealed by
491 metagenomic analysis. *Environmental Microbiology* n/a.
- 492 23. Zhang M, Li Z, Häggblom MM, Young L, He Z, Li F, Xu R, Sun X, Sun W. 2020. Characterization of
493 nitrate-dependent As(III)-oxidizing communities in arsenic-contaminated soil and investigation of their
494 metabolic potentials by the combination of DNA-stable isotope probing and metagenomics. *Environmental*
495 *Science & Technology* 54:7366-7377.
- 496 24. Garcia-Dominguez E, Mumford A, Rhine ED, Paschal A, Young LY. 2008. Novel autotrophic
497 arsenite-oxidizing bacteria isolated from soil and sediments. *FEMS Microbiology Ecology* 66:401-410.
- 498 25. Tratnyek PG, Grundl TJ, Haderlein SB. 2011. Aquatic redox chemistry. ACS Publications.
- 499 26. Hu Y, Wu G, Li R, Xiao L, Zhan X. 2020. Iron sulphides mediated autotrophic denitrification: An
500 emerging bioprocess for nitrate pollution mitigation and sustainable wastewater treatment. *Water Research*
501 179:115914.
- 502 27. Hayat K, Menhas S, Bundschuh J, Chaudhary HJ. 2017. Microbial biotechnology as an emerging
503 industrial wastewater treatment process for arsenic mitigation: A critical review. *Journal of Cleaner*
504 *Production* 151:427-438.
- 505 28. Jousset A, Bienhold C, Chatzinotas A, Gallien L, Gobet A, Kurm V, Küsel K, Rillig MC, Rivett DW,
506 Salles JF, van der Heijden MGA, Youssef NH, Zhang X, Wei Z, Hol WHG. 2017. Where less may be more:
507 how the rare biosphere pulls ecosystems strings. *The ISME journal* 11:853.
- 508 29. Straub KL, Benz M, Schink B, Widdel F. 1996. Anaerobic, nitrate-dependent microbial oxidation of
509 ferrous iron. *Applied and Environmental Microbiology* 62:1458.
- 510 30. Schippers A, Jørgensen BB. 2002. Biogeochemistry of pyrite and iron sulfide oxidation in marine
511 sediments. *Geochimica et Cosmochimica Acta* 66:85-92.
- 512 31. Beller HR. 2005. Anaerobic, nitrate-dependent oxidation of U(IV) oxide minerals by the
513 chemolithoautotrophic bacterium *Thiobacillus denitrificans*. *Applied and Environmental Microbiology*

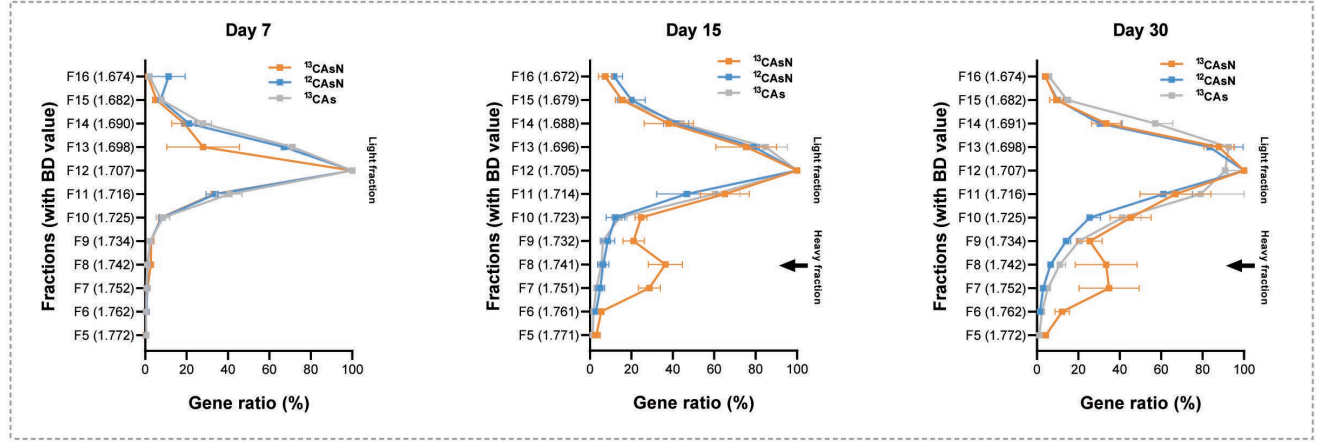
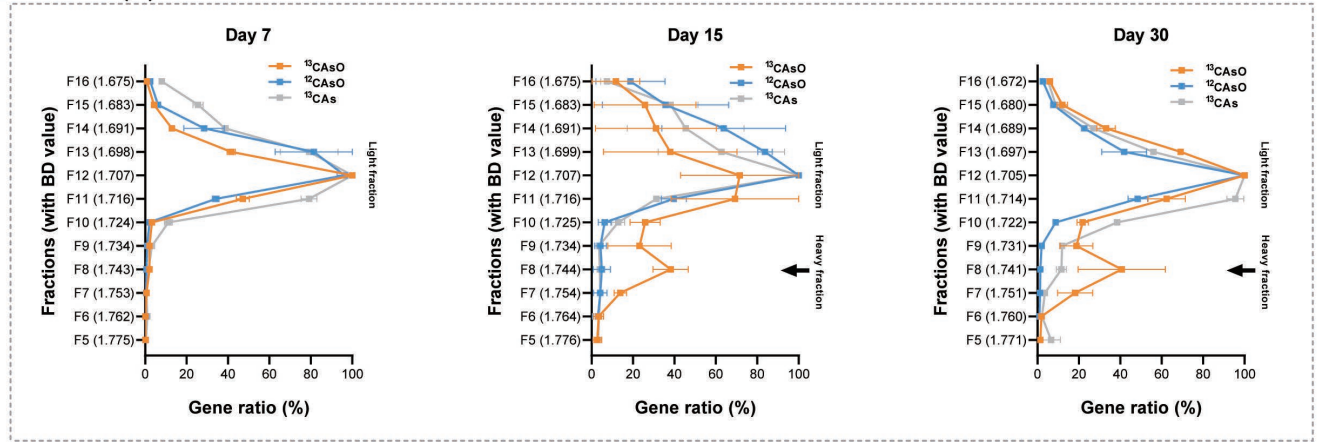
- 514 71:2170-4.
- 515 32. Qin J, Rosen BP, Zhang Y, Wang G, Franke S, Rensing C. 2006. Arsenic detoxification and evolution of
516 trimethylarsine gas by a microbial arsenite S-adenosylmethionine methyltransferase. *PNAS* 103:2075.
- 517 33. vanden Hoven RN, Santini JM. 2004. Arsenite oxidation by the heterotroph *Hydrogenophaga* sp. str.
518 NT-14: the arsenite oxidase and its physiological electron acceptor. *Biochimica et Biophysica Acta*
519 1656:148-155.
- 520 34. Fan X, Nie L, Shi K, Wang Q, Xia X, Wang G. 2019. Simultaneous 3-/4-Hydroxybenzoates
521 Biodegradation and Arsenite Oxidation by *Hydrogenophaga* sp. H7. *Frontiers in Microbiology* 10.
- 522 35. Willems A, Gillis M. 2015. *Hydrogenophaga*. *Bergey's Manual of Systematics of Archaea and*
523 *Bacteria*:1-15.
- 524 36. Yoon I-H, Chang J-S, Lee J-H, Kim K-W. 2009. Arsenite oxidation by *Alcaligenes* sp. strain RS-19
525 isolated from arsenic-contaminated mines in the Republic of Korea. *Environmental Geochemistry and*
526 *Health* 31:109.
- 527 37. Escalante G, Campos VL, Valenzuela C, Yañez J, Zaror C, Mondaca MA. 2009. Arsenic resistant
528 bacteria isolated from arsenic contaminated river in the Atacama Desert (Chile). *Bulletin of Environmental*
529 *Contamination and Toxicology* 83:657-661.
- 530 38. Banerjee S, Schlaeppli K, Mga VDH. 2018. Keystone taxa as drivers of microbiome structure and
531 functioning. *Nature Reviews Microbiology* 16:1.
- 532 39. Xu R, Li B, Xiao E, Young LY, Sun X, Kong T, Dong Y, Wang Q, Yang Z, Chen L, Sun W. 2020.
533 Uncovering microbial responses to sharp geochemical gradients in a terrace contaminated by acid mine
534 drainage. *Environmental Pollution* 261:114226.
- 535 40. Sun X, Xu R, Dong Y, Li F, Tao W, Kong T, Zhang M, Qiu L, Wang X, Sun W. 2020. Investigation of
536 the ecological roles of putative keystone taxa during tailing revegetation. *Environmental Science &*
537 *Technology* 54:11258-11270.
- 538 41. Tyc, Olaf, Song C, Dickschat JS, Vos M, Garbeva P. 2017. The ecological role of volatile and soluble
539 secondary metabolites produced by soil bacteria. *Trends in Microbiology* 25:280-292.
- 540 42. Riley MA, Wertz JE. 2002. Bacteriocins: evolution, ecology, and application. *Annual Review of*
541 *Microbiology* 56:117-137.
- 542 43. Hutt LP, Huntemann M, Clum A, Pillay M, Palaniappan K, Varghese N, Mikhailova N, Stamatis D,
543 Reddy T, Daum C. 2017. Permanent draft genome of *Thiobacillus thioparus* DSM 505 T, an obligately
544 chemolithoautotrophic member of the Betaproteobacteria. *Standards in Genomic Sciences* 12:10.
- 545 44. Martin-Creuzburg D, Beck B, Freese HM. 2011. Food quality of heterotrophic bacteria for *Daphnia*
546 magna: evidence for a limitation by sterols. *FEMS Microbiology Ecology* 76:592-601.
- 547 45. Mishra J, Arora NK. 2018. Secondary metabolites of fluorescent pseudomonads in biocontrol of
548 phytopathogens for sustainable agriculture. *Applied Soil Ecology* 125:35-45.
- 549 46. Clements T, Ndlovu T, Khan W. 2019. Broad-spectrum antimicrobial activity of secondary metabolites
550 produced by *Serratia marcescens* strains. *Microbiological Research* 229:126329.
- 551 47. Sheng G, Yu H, Li X. 2010. Extracellular polymeric substances (EPS) of microbial aggregates in
552 biological wastewater treatment systems: A review. *Biotechnology Advances* 28:882-894.
- 553 48. Hansen SK, Rainey PB, Haagenensen JA, Molin S. 2007. Evolution of species interactions in a biofilm

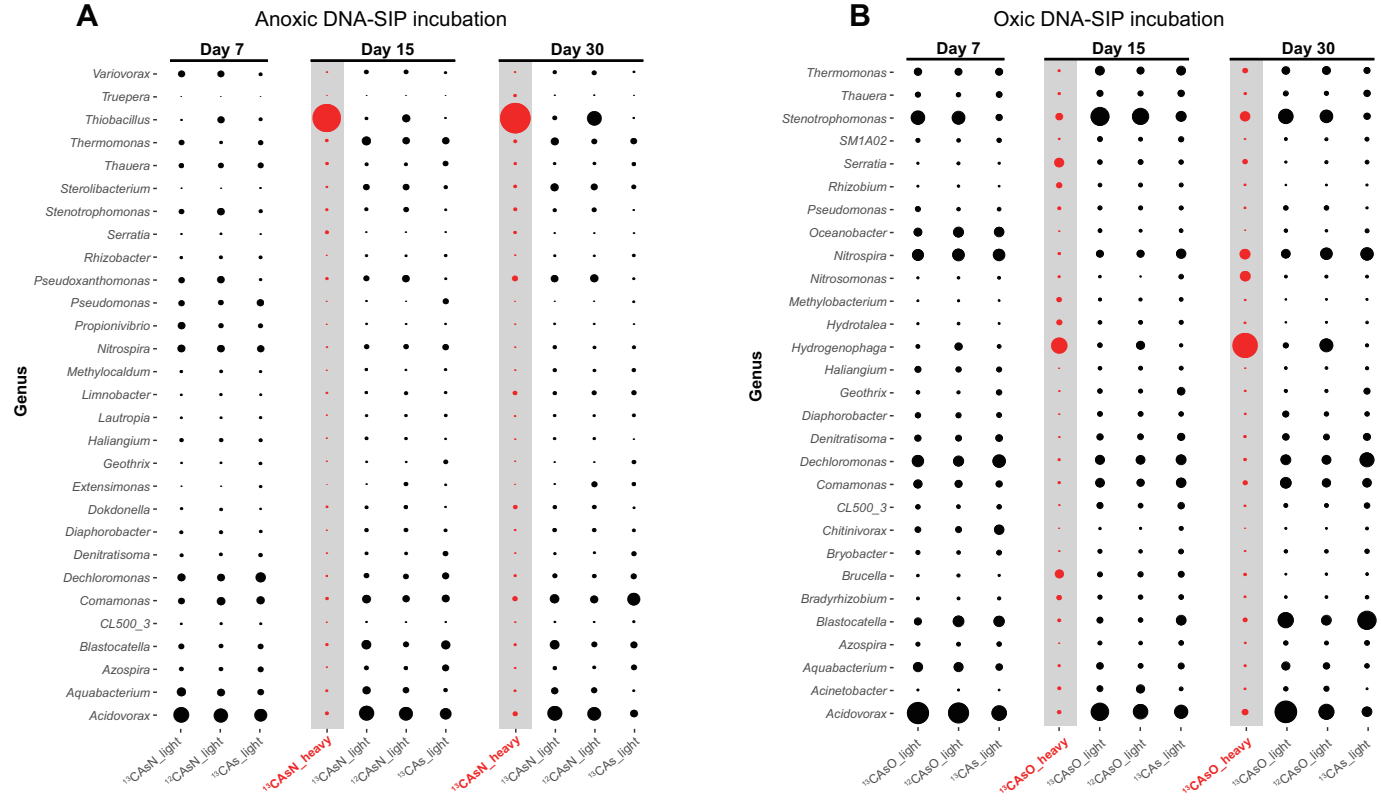
- 554 community. *Nature* 445:533-6.
- 555 49. Xu R, Zhang Y, Xiong W, Sun W, Fan Q, Zhaohui Y. 2020. Metagenomic approach reveals the fate of
556 antibiotic resistance genes in a temperature-raising anaerobic digester treating municipal sewage sludge.
557 *Journal of Cleaner Production* 277:123504.
- 558 50. Xu R, Yang Z, Zheng Y, Zhang H, Liu J, Xiong W, Zhang Y, Ahmad K. 2017. Depth-resolved microbial
559 community analyses in the anaerobic co-digester of dewatered sewage sludge with food waste. *Bioresource*
560 *Technology* 244:824-835.
- 561 51. Quéméneur M, Cébron A, Billard P, Battaglia-Brunet F, Garrido F, Leyval C, Joulian C. 2010.
562 Population structure and abundance of arsenite-oxidizing bacteria along an arsenic pollution gradient in
563 waters of the Upper Isle River Basin, France. *Applied and Environmental Microbiology* 76:4566-4570.
- 564 52. Zhang J, Zhou W, Liu B, He J, Shen Q, Zhao F-J. 2015. Anaerobic arsenite oxidation by an autotrophic
565 arsenite-oxidizing bacterium from an arsenic-contaminated paddy soil. *Environmental Science &*
566 *Technology* 49:5956-5964.
- 567 53. Xu R, Yang Z, Wang Q, Bai Y, Liu J, Zheng Y, Zhang Y, Xiong W, Ahmad K, Fan C. 2018. Rapid
568 startup of thermophilic anaerobic digester to remove tetracycline and sulfonamides resistance genes from
569 sewage sludge. *Science of The Total Environment* 612:788-798.
- 570 54. Sun W, Sun X, Li B, Xu R, Young LY, Dong Y, Zhang M, Kong T, Xiao E, Wang Q. 2020. Bacterial
571 response to sharp geochemical gradients caused by acid mine drainage intrusion in a terrace: Relevance of C,
572 N, and S cycling and metal resistance. *Environment International* 138:105601.
- 573 55. Bolger AM, Lohse M, Usadel B. 2014. Trimmomatic: a flexible trimmer for Illumina sequence data.
574 *Bioinformatics* 30:2114-2120.
- 575 56. Xu R, Zhang M, Lin H, Gao P, Yang Z, Wang D, Sun X, Li B, Wang Q, Sun W. 2022. Response of soil
576 protozoa to acid mine drainage in a contaminated terrace. *Journal of Hazardous Materials* 421:126790.
- 577 57. Li D, Liu C-M, Luo R, Sadakane K, Lam T-W. 2015. MEGAHIT: an ultra-fast single-node solution for
578 large and complex metagenomics assembly via succinct de Bruijn graph. *Bioinformatics* 31:1674-1676.
- 579 58. Gherman U, Jocelyne D, James T. 2018. MetaWRAP-a flexible pipeline for genome-resolved
580 metagenomic data analysis. *Microbiome*.
- 581 59. Parks DH, Imelfort M, Skennerton CT, Hugenholtz P, Tyson GW. 2015. CheckM: assessing the quality
582 of microbial genomes recovered from isolates, single cells, and metagenomes. *Genome Research*
583 25:1043-1055.
- 584 60. Sun X, Qiu L, Kolton M, Haegglblom M, Xu R, Kong T, Gao P, Li B, Jiang C, Sun W. 2020. VV
585 reduction by *Polaromonas* spp. in vanadium mine tailings. *Environmental Science & Technology*.
- 586 61. Chaumeil PA, Mussig AJ, Hugenholtz P, Parks DH. 2019. GTDB-Tk: a toolkit to classify genomes with
587 the Genome Taxonomy Database. *Bioinformatics* 36:1925-7.
- 588 62. Aramaki T, Blanc-Mathieu R, Endo H, Ohkubo K, Kanehisa M, Goto S, Ogata H. 2020. KofamKOALA:
589 KEGG Ortholog assignment based on profile HMM and adaptive score threshold. *Bioinformatics*
590 36:2251-2252.
- 591 63. Sun X, Song B, Xu R, Zhang M, Gao P, Lin H, Sun W. 2021. Root-associated (rhizosphere and
592 endosphere) microbiomes of the *Miscanthus sinensis* and their response to the heavy metal contamination.
593 *Journal of Environmental Sciences* 104:387-398.
- 594 64. Xu R, Yang Z, Zheng Y, Liu J, Xiong W, Zhang Y, Lu Y, Xue W, Fan C. 2018. Organic loading rate and

- 595 hydraulic retention time shape distinct ecological networks of anaerobic digestion related microbiome.
596 *Bioresource Technology* 262:184-193.
- 597 65. Xu R, Sun X, Lin H, Han F, Xiao E, Li B, Qiu L, Song B, Yang Z, Sun W. 2020. Microbial adaptation in
598 vertical soil profiles contaminated by an antimony smelting plant. *FEMS Microbiology Ecology* 96:1-12.
- 599

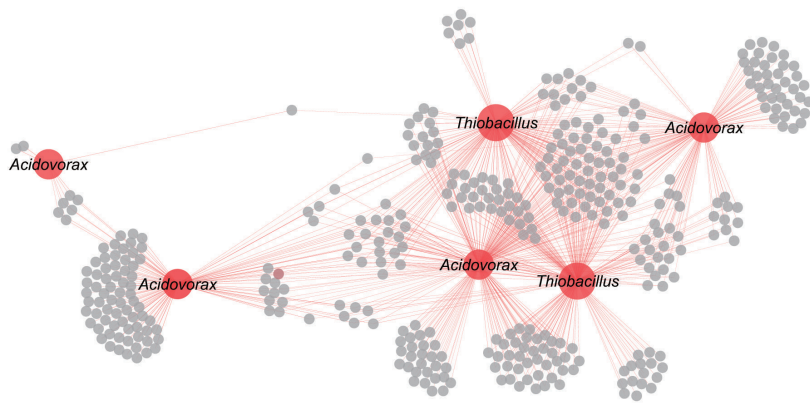
A**B**



A Anoxic As(III) oxidation**B** Oxidic As(III) oxidation

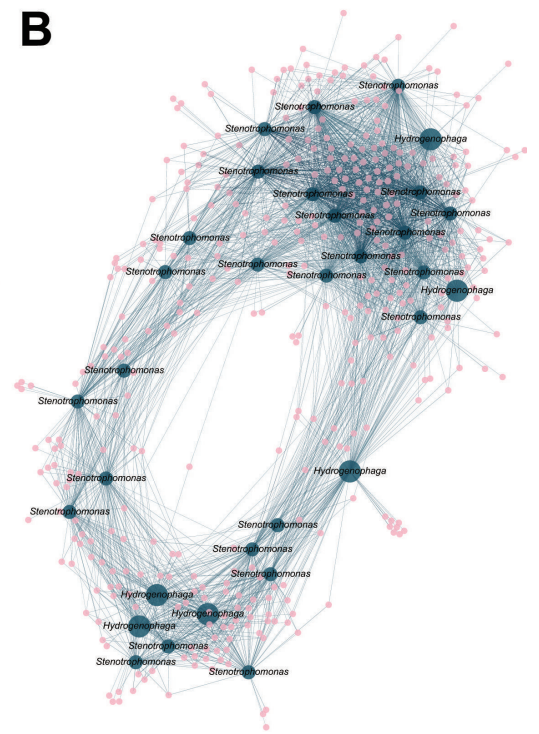


A



Anoxic network

B



Oxic network

